Supplementary Information for:

Uncoupling of the endocannabinoid signaling complex in a mouse model of fragile X syndrome

Kwang-Mook Jung[1,#], Marja Sepers[2,3,#], Christopher M. Henstridge[4,#], Olivier Lassalle[6,7,8], Daniela Neuhofer[6,7,8], Henry Martin[6,7,8], Melanie Ginger[2,3], Andreas Frick[2,3], Nicholas V. DiPatrizio[1], Ken Mackie[5], Istvan Katona[4°], Daniele Piomelli[1,9,10,°] and Olivier J. Manzoni[2,3,6,7,8,°].

[#] These authors contributed equally to this study.

°Corresponding authors.

[1] Department of Pharmacology, University of California, Irvine, Irvine, CA 92697, USA.

[2] INSERM U862, Physiopathology of Synaptic Plasticity Group, Neurocentre Magendie, 146 Rue Léo-Saignat, F 33077 Bordeaux Cedex, France.

[3] University of Bordeaux, Bordeaux, F 33077, France.

[4] Institute of Experimental Medicine, Hungarian Academy of Sciences, H-1083 Budapest, Hungary.

[5] Department of Psychological and Brain Sciences, Gill Center for Biomolecular Science, Indiana University, Bloomington, IN 47405, USA.

[6] INSERM U901, Marseille, 13009, France.

[7] Université de la Méditerranée UMR S901 Aix-Marseille 2, France.

[8] INMED, Marseille, 13009, France.

[9] Department of Biological Chemistry, University of California, Irvine, Irvine, CA 92697, USA.

[10] Unit of Drug Discovery and Development, Italian Institute of Technology, Genova, 16163, Italy.

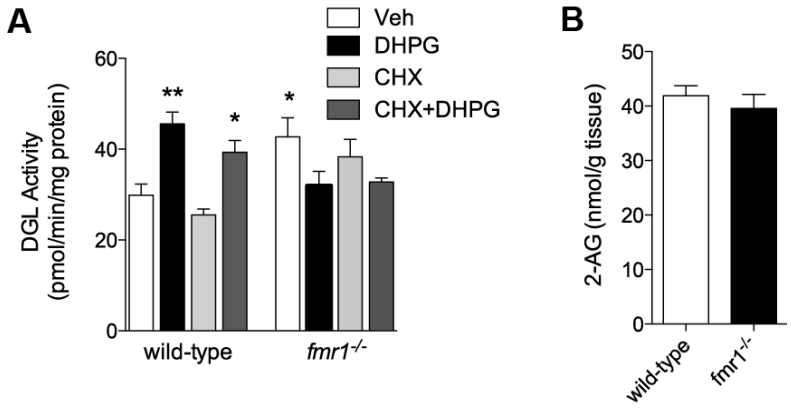

Supplementary Figure S1. DHPG stimulates DGL activity in a protein synthesis-independent mechanism.

A. Synaptoneurosomes fractions (SN, 1 mg/ml) prepared from wild-type or *fmr1*$^{-/-}$ mice on C57BL/6J background were pre-treated with vehicle (Veh, water) or cycloheximide (10 µg/ml, CHX) for 5 min at 37 ℃ and incubated with DHPG (100 µM) for additional 30 min. Then, DGL activity was measured *in vitro* for 15 min using 10 µM diheptadecanoylglycerol as a substrate (n=4). **B.** 2-AG levels were quantified from dissected frontal cortex of wild-type or *fmr1*$^{-/-}$ mice on FVB.129 background using a LC/MS method, as described in *Experimental Procedures* (n=6). Results are representative of at least two independent experiments. Significance was determined using two-tailed Student's t test. **P*<0.05 and ***P*<0.01. Error bars represent S.E.M.

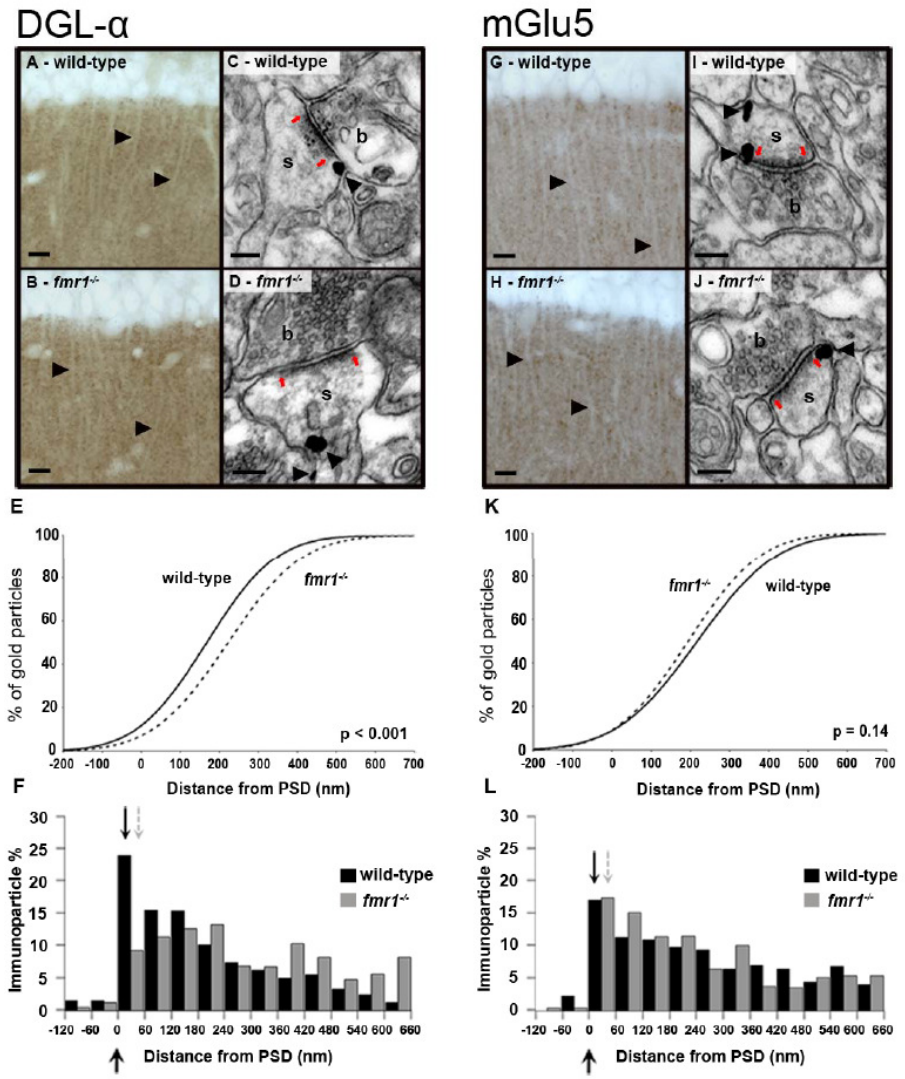

Supplementary Figure S2. Impaired targeting of DGL-α to excitatory synapses in the hippocampus of *fmr1*$^{-/-}$ mice.

DGL-α localization in wild-type and *fmr1*$^{-/-}$ mice. (**A, B**). Light micrographs of DGL-α immunoperoxidase labeling in wild-type (**A**) and *fmr1*$^{-/-}$ mice (**B**). The granular staining of DGL-α-immunoreactivity found within the neuropil of the hippocampus suggests a compartmentalized localization of the enzyme in wild-type and *fmr1*$^{-/-}$ mice. Apical dendrites of CA1 pyramidal neurons are largely devoid of labeling (arrowheads). (**C, D**) Electron micrographs of asymmetric synapses displaying DGL-α-immunogold labeling, in wild-type (**C**) and *fmr1*$^{-/-}$ mice (**D**). Gold particles representing the precise localization of DGL-α (white arrowheads) are predominantly found in the perisynaptic domain close to the PSD (small red arrows) in wild-type animals, whereas in *fmr1*$^{-/-}$ animals, gold particles are usually found in more distal locations from the PSD. s – spine head, b – bouton. (**E**) Cumulative distribution plot of DGL-α-immunogold particles in wild-type (solid line, n = 300), and *fmr1*$^{-/-}$ mice (dashed line, n = 300). (**F**) Histogram summarizing the skewed perisynaptic distribution of normalized DGL-α-immunogold particles on the plasma membrane of dendritic spine heads in wild-type mice (black arrow and black bars, n = 300), and the lack of biased distribution in *fmr1*$^{-/-}$ mice (grey arrow and grey bars, n = 300). Large black arrow below represents the edge of the PSD. (**G, H**) Light micrographs of $mGlu_5$ immunoperoxidase labeling in wild-type (**G**) and *fmr1*$^{-/-}$ animals (**H**). $mGlu_5$-immunoreactivity displays a similar granular pattern within the neuropil as DGL-α, with apical dendrites of CA1 pyramidal cells largely devoid of labeling (arrowheads). (**I, J**) Electron micrographs of asymmetric synapses displaying $mGlu_5$-immunogold labeling (arrowhead), in wild-type (**I**) and *fmr1*$^{-/-}$ animals (**J**). In contrast to DGL-α localization, $mGlu_5$ was predominantly found in the perisynaptic domain adjacent to the PSD (small red arrows) in both wild-type and *fmr1*$^{-/-}$ mice. s – spine head, b – bouton. (**K**) Cumulative distribution plot of $mGlu_5$-immunogold particles in wild-type (solid line, n = 300), and *fmr1*$^{-/-}$ mice (dashed line, n = 300). (**L**) Histogram representing the similar normalized distribution of $mGlu_5$-immunogold particles on dendritic spine heads in wild-type (black arrow and black bars, n = 300) and *fmr1*$^{-/-}$ animals (grey arrow and grey bars, n = 300). Large black arrow below histogram points to the edge of the PSD. Scale bars: 15 μm in A, B, G, H and 100 nm in C, D, I , J.

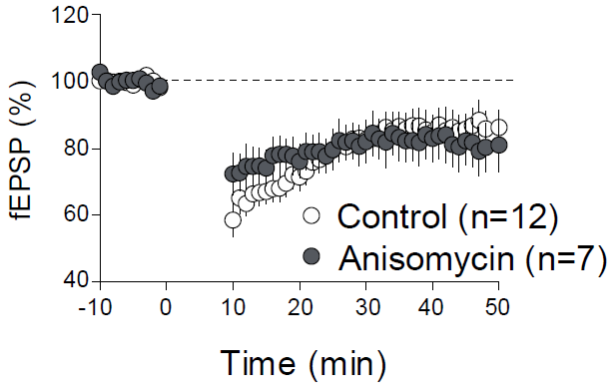

Supplementary Figure S3. eCB-LTD is independent on protein synthesis.
Normalized fEPSP amplitude in wild-type mice without (white symbols) or with anisomycin (30 μM; grey symbols) pretreatment (starting 45-90 min prior to LTD induction) followed by the LTD induction protocol at time zero. Error bars represent S.E.M.

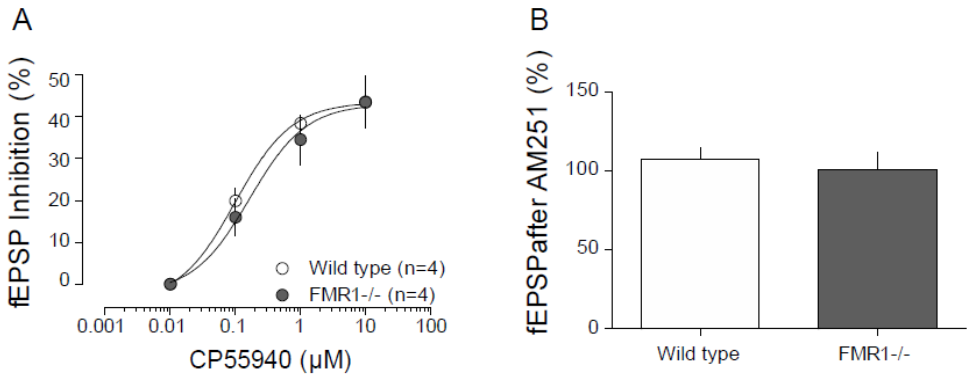

Supplementary Figure S4. Effects of CB_1 receptors activation and tonic eCB release are unchanged in *fmr1*$^{-/-}$ mice.

A. Dose response curves for the cannabinoid agonist CP55940 in wild-type and *fmr1*$^{-/-}$ littermates (NS). **B.** fEPSP amplitudes measured 20-25 min after application of the CB1 receptor antagonist AM251 (4 µM), normalized to baseline, show no change in tonic eCB release between wild-type and *fmr1*$^{-/-}$ mice (NS). Error bars represent S.E.M.

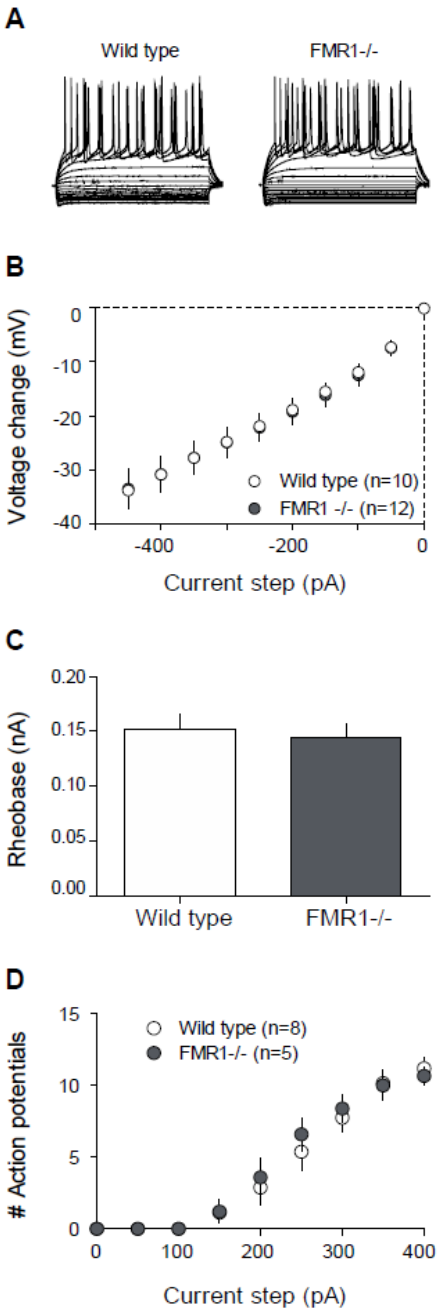

Supplementary Figure S5. Similar intrinsic excitability of ventral striatum medium spiny neurons from wild-type or *fmr1*$^{-/-}$ mice.

A. Typical membrane responses to somatic current steps of medium spiny ventral striatum neurons from wild-type (left) or *fmr1*$^{-/-}$ (right) mice. **B.** Summary current–voltage (I–V) curves from wild-type (white symbols, n=10) or *fmr1*$^{-/-}$ (filled symbols, n=12) medium spiny neuron. **C.** The rheobase was identical in both mice groups (*fmr1*$^{-/-}$, grey bar; wild-type, white bar). **D.** Summary of current-firing curves indicate that the number of evoked action potentials in response to somatic current steps were identical in medium spiny neurons from both phenotypes (wild-type n=8, white symbols; *fmr1*$^{-/-}$ n=5, grey symbols). Error bars represent S.E.M.

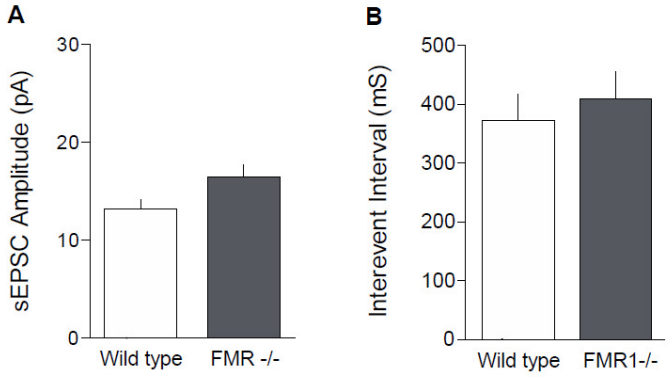

Supplementary Figure S6. Basal excitatory transmission is normal in *fmr1*$^{-/-}$ mice.
A. The median AMPAR spontaneous miniature EPSCs (sEPSCs) amplitudes recorded at -70 mV in medium spiny neurons from wild-type and *fmr1*$^{-/-}$ mice were undistinguishable ($P > 0.05$, Mann Whitney U test). **B.** No changes were observed in the median interevent intervals of AMPAR sEPSCs (*fmr1*$^{-/-}$, grey bars; wild-type, white bars). Error bars represent S.E.M.

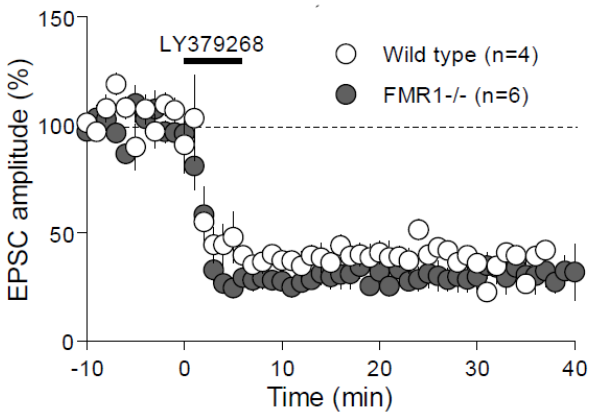

Supplementary Figure S7. The presynaptic LTD machinery is functional in *fmr1*$^{-/-}$ mice.
Normalized fEPSP amplitude showing that LTD induced by bath application of the $mGluR_{2/3}$ specific agonist LY379268 (100 nM, 5 min) is normal in *fmr1*$^{-/-}$ mice (*fmr1*$^{-/-}$, grey symbols; wild-type, white symbols). Error bars represent S.E.M.

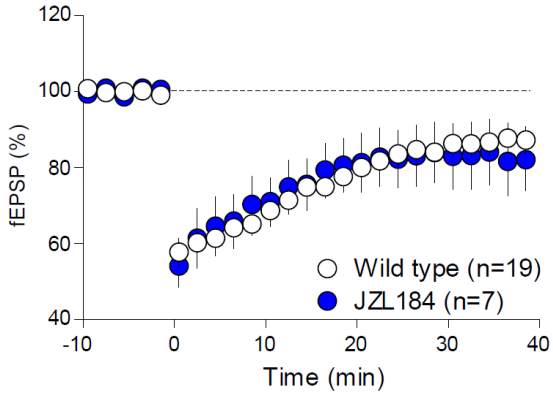

Supplementary Figure S8. Blocking of 2-AG degradation has no effect on LTD in wild-type mice.
Normalized fEPSP amplitude in wild-type mice without (white symbols) or with JZL184 (1 μM; blue symbols) pretreatment (starting 45-90 min prior to LTD induction) followed by the LTD induction protocol at time zero. Error bars represent S.E.M.

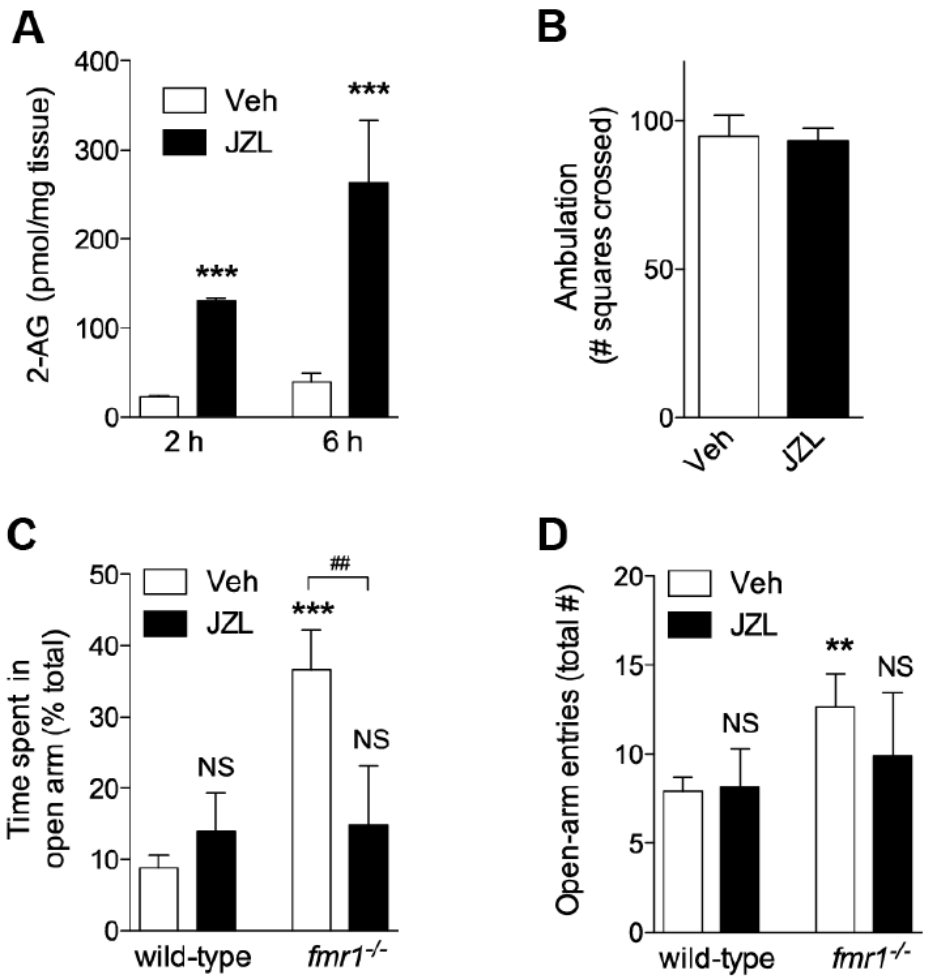

Supplementary Figure 9. Effects of JZL184 on genotypic behaviors of *fmr1*$^{-/-}$ mice.
A. JZL184 (JZL, 16 mg/kg) or vehicle was administered by i.p. to adult male C57BL/6J mice. Brains were isolated at the indicated time and 2-AG levels were quantified by liquid chromatography/mass spectrometry (n=3-4). ***P<0.001 compared to Veh, by two-tailed Student's t test. **B.** Effects of JZL184 on locomotive activity of adult male C57BL/6 mice were determined by open field test, after 6 h from i.p. injection of JZL184 (16 mg/kg) or vehicle (n=5). **C**-**D.** Elevated plus maze behaviors of wild-type or *fmr1*$^{-/-}$ mice. Mice were administered with MGL inhibitor JZL184 (JZL, 16 mg/kg) or vehicle (Veh) and subjected to elevated plus maze test after 6 hr from the injection. Percent of time spent in open arm (**C**) and total open are entries (**D**) were counted. Significance was determined using two-way ANOVA with post-hoc Student-Newman-Keuls test. NS, not significant; **P<0.01 and ***P<0.001 compared to wild-type-Veh; $^{\#\#}P$<0.01 compared to *fmr1*$^{-/-}$ -Veh (n=11 per each group). Error bars represent S.E.M.

Supplementary Methods:

Electrophysiology:

Whole cell patch-clamp of visualized medium spiny neurons, prefrontal cortex pyramidal neurons and field potential recordings were made in coronal slices containing the ventral striatum or the prefrontal cortex as previously described [8, 9]. Medium spiny neurons (MSN) were identified using morphological characteristics (kidney-like flat shape, medium size). Recordings were made in the medial ventral accumbens core close to the anterior commissure or in pyramidal cells layers 5/6 of the prefrontal cortex as described previously [8, 9, 46]. For recording, slices were placed in the recording chamber and superfused (1.5 - 2 ml/min) with ACSF (same as low Ca – ACSF with the following exception: 2.4 mM $CaCl_2$ and 1.2 mM $MgCl_2$). All experiments were done at room temperature. The superfusion medium contained picrotoxin (100 µM) to block gamma-aminobutyric acid type A (GABA-A) receptors. All drugs were added at the final concentration to the superfusion medium, with the exception of JZL184 and THL, which were added to the solution before recording.

For whole cell patch-clamp experiments, neurons were visualized using an upright microscope with infrared illumination. Two intracellular solutions were used, based on cesium methane-sulfonate (for voltage clamp) or K^+ gluconate (for current clamp), as follows (in mM): 128 cesium methane-sulfonate (CH_3O_3SCs) or K^+ gluconate, 20 NaCl, 1 $MgCl_2$, 1 EGTA, 0.3 $CaCl_2$, 2 Na_2^+ATP, and 0.3 Na^+ GTP, buffered with 10 HEPES, pH 7.2, osmolarity 290-300 mOsm. Electrode resistance was 4-6 MOhms. A –2 mV hyperpolarizing pulse was applied before each evoked EPSC in order to evaluate the access resistance, and those experiments in which this parameter changed >20% were rejected. Access resistance compensation was not used and acceptable access resistance was <25 MOhms. The potential reference of the amplifier was adjusted to zero prior to breaking into the cell. Whole cell patch-clamp recording were performed with an Axopatch-200B (Molecular Device, Sunnyvale, USA). Data were filtered at 1-2 kHz, digitized at 10 kHz on a DigiData 1332A interface (Molecular Device, Sunnyvale, USA) and collected on a PC using Clampex 9.

For extracellular field experiments (fEPSP), the recording pipette was filled with ACSF. Both the fEPSP amplitude and area were measure (graphs depict amplitudes). To evoke synaptic currents, stimuli (100 µsec duration) were delivered at 0.1 Hz with a glass electrode filled with ACSF and placed at a distance > 150 mM in the dorsomedial direction (ventral striatum recordings) or in pyramidal cells layer 2/3 (prefrontal cortex recordings). The extracellular fEPSP was confirmed to be glutamatergic by application at the end of the experiments of the non-NMDA ionotropic glutamate receptor antagonist, DNQX (20 µM), completely blocking the synaptic component.

Current voltage (I-V) curves MSN were made by a series of hyperpolarizing to depolarizing current steps immediately after breaking into the cell. Membrane resistance was estimated

from the *I–V* curve around resting membrane potential (RMP) [47]. Spontaneous EPSCs (sEPSCs) were recorded at -70 mV in whole cell voltage clamp configuration using Axoscope 10 (Molecular Devices). A template was made with Clampfit 10 (Molecular Devices) by averaging several typical synaptic events and sEPSCs detected with a lower threshold of -6 mV.

Biochemistry:

Reverse Transcriptase-PCR and Quantitative PCR:

We extracted total RNA with TRIzol (Invitrogen, Carlsbad, CA)-RNeasy (Qiagen) hybrid method, and synthesized first-strand complementary DNA using SuperScript II RNaseH reverse transcriptase (Invitrogen). Reverse transcription of total RNA (2 μg) was carried out using oligo(dT)12–18 primers for 50 min at 42°C. Real-time quantitative PCR was conducted using an Mx3000P system (Stratagene). We designed primer/probe sets with Primer Express software (Applied Biosystems, Foster City, CA) and mouse DGL-α sequence obtained from NCBI database (GenInfo Identifier 37674270). Primers and fluorogenic probes were synthesized by TIB Molbiol (Adelphia, NJ). DGL-α mRNA levels were normalized using glyceraldehyde-3-phosphate dehydrogenase as an internal standard. The primer/probe sequences for DGL-α were: forward, 5′-CCAGGCCTTTGGGCG-3′; reverse, 5′ GCCTACCACAATCAGGCCAT-3′; and TaqMan probe, 5′-ACCTGGGCCGTGGAACCAAACA-3′. We used TaqMan gene expression assays for mouse PSD-95 (Mm00492193_m1) and APP (Mm01344172_m1) (Applied Biosystems).

Immunoprecipitation:

We removed whole brains from wild-type and *fmr1*$^{-/-}$ *mice*, and homogenized them in 10 ml of ice-cold immunoprecipitation (IP) buffer [20 mM Tris-pH7.4, 200 mM NaCl, 30 mM EDTA, 0.5% Triton-X100, 1x protease inhibitor (Roche), 20 units/ml RNase inhibitor (Promega)] [49]. After centrifuging at 3,000 x g for 10 min, the supernatants were brought to 400 mM NaCl, and then centrifuged again at 70,000 x g for 30 min. The resulting supernatant was cleared by incubation with protein G-sepharose (GE Healthcare, Piscataway, NJ) coated with bovine serum albumin for 1 hr, and the cleared supernatant was immunoprecipitated with an anti-FMRP antibody. After overnight incubation at 4 °C, 50 μl of protein G-Sepharose was added and further incubated for 1 hr. The immunoprecipitates were washed six times with IP buffer, eluted with SDS sample buffer or Trizol to be used for protein analysis and RNA extraction, respectively [50].

Protein Measurements:

Western blot analyses were conducted as described (Jung et al., 2007). We used rabbit polyclonal anti-DGL-α (1:1,000, "INT"; [13]), monoclonal anti-FMRP (1:1,000; Millipore), monoclonal anti-$mGlu_5$ (1:1,000, Millipore) or monoclonal anti-Actin (1:2,000; Sigma-Aldrich) as primary antibodies.

DGL Assay:

DGL activity was measured at 37°C for 30 min in 50 mM Tris-HCl, pH 7.0, containing 0.1% Triton X-100, tissue homogenate protein (100 µg) and 1,2-diheptadecanoyl-*sn*-glycerol (Nu-Chek Prep, 50 µM) as substrate. The reactions were stopped by adding chloroform-methanol (1:1) containing [$^2H_8$]-2-AG. After centrifugation at 3000 x g at 4°C for 15 min, the organic layers were collected and dried under N_2. The residues were suspended in chloroform/methanol (1:3, 50 µl) and analyzed by LC/MS. For quantification purposes, we monitored the reaction product heptadecanoyl-*sn*-glycerol $[M^+Na]^+$ (m/z 367) along with standard [$^2H_8$]2-AG (m/z 409).

Statistical Analyses:

Results are expressed as the mean ± S.E.M. Statistical significance was evaluated using the Student's *t* test.

Animal Behaviour:

Adult male *fmr1*$^{-/-}$ C57BL/6J mice were used for the animal behavior studies.

Open field & Elevated plus maze:

The open-field apparatus and procedure were based off of previously published methods [51]. The open field was constructed with black Plexiglas (50 x 50 x 40 cm high) and the floor of the apparatus was marked with black lines giving 9 squares, each 16.7 cm x 16.7 cm. These markings were made on the underside of a clear Plexiglas floor panel and lined with white plastic film to give appropriate contrast between the animal and floor for detection with the video tracking system. Lighting consisted of four 25 watts fluorescent bulbs at a height of 2 m above the floor of the open field apparatus. The floor was cleaned with a 10% ethanol solution between each trial. The animals were placed in the center square and allowed to freely explore the test apparatus for 5 min. The total distance traveled, as well as total number of squares crossed (ambulation), were quantified by Ethovision 3.1 video tracking system.

Elevated plus maze:

The elevated plus maze and procedure were based off of previously published methods [52]. The maze was constructed of black plexiglass and consisted of two open arms (30 x 5cm) and closed arms (30 x 5cm, with 15cm side panels on closed arms). The arms were lined with white plastic film to give appropriate contrast between the animal and Plexiglas floor for detection with the video tracking system. The arms extended from a center square (5 x 5 cm). The maze was mounted on a Plexiglas base and raised 39 cm above the ground. Lighting consisted of two 40W incandescent bulbs, each hanging at a height of 1 m above the open arms of the test apparatus. The floor of the apparatus was cleaned with a 10% ethanol solution between each trial. The animals were placed in the center square and allowed to freely explore for 5 min. The amount of time spent in each arm and the number of entries into each arm were quantified by Ethovision 3.1 video tracking system (Noldus, Netherlands).

Anatomy:

Quantitative analysis of the distribution of DGL-α and mGlu$_5$ in dendritic spines: Supplementary Methods

To establish the precise subcellular distribution of DGL-α and mGlu$_5$ within dendritic spines, high-resolution quantitative evaluation was performed in a population of 100-100 immunogold-labeled dendritic spine heads from each animal. Samples for electron microscopic analysis were taken from the core region of the ventral striatum. Superficial ultrathin sections (first ≈ 5 μm) were collected to ensure equal probability of antibody penetration, which decreases with depth. To be able to compare the distribution of DGL-α and mGlu$_5$ along the plasma membrane surface of dendritic spine heads, we followed a similar analysis procedure of Lujan and colleagues [14, 53]. Briefly, the localization of the gold particles was measured as the distance between the closest edge of the postsynaptic density (PSD) and the center of the immunoparticles present on the plasma membrane of the spines. Gold particles were considered to be membrane-associated if located intracellularly within 40 nm of the plasma membrane. The distribution of gold particles was found to be similar between animals of the same group (Kolmogorov-Smirnov test; $P > 0.05$); hence subsequently data was pooled in each group. The distribution of gold particles between wild-type and FMRP knockout animals was also compared with the Kolmogorov-Smirnov test and significance was assumed if $P < 0.05$. In the case of DGL-α-immunogold labeling, a second analysis was also carried out to unequivocally confirm that the shape of the distributions were distinct. The measured distance values were standardized by subtracting the mean value and normalizing to the standard deviation of 1. This new dataset was compared with Kolmogorov-Smirnov test, which indeed revealed distinct distributions in wild-type and *fmr1*$^{-/-}$ animals ($P = 0.028$). Previous studies in other brain regions of *fmr1*$^{-/-}$ mice have reported various alterations in spine density and length [54], which may have potentially confounded the distribution of postsynaptic proteins. To determine spine size and shape in our samples, we have compared some characteristic parameters. First, the average length of the postsynaptic density was not changed (Kolmogorov-Smirnov test ($P = 0.096$); wild-type: 275 ± 5 nm, *fmr1*$^{-/-}$: 287 ± 6 nm) and was similar to the data published previously in mouse and rat hippocampus [13, 14]. To assess the length of plasma membrane of the spine heads, the perimeter of each spine head was measured and the length of the PSD subtracted. Assuming the spine head exists as a “ball” shape in 3-dimensions, the perimeter was halved to find the true length of membrane from the edge of PSD to base of spine neck. These lengths were compared between wild-type and *fmr1*$^{-/-}$ animals with Kolmogorov-Smirnov test ($P = 0.002$). To normalize for this difference we used the normalization approach described by Lujan et al., 1996. The total length of spine membrane was measured for every DGL-α-positive or mGlu$_5$-positive spine and divided into 60 nm bins. Because the samples from three animals did not differ significantly in each group, data were pooled and expressed as

the proportion of gold particle-containing plasma membrane divisions. The occurrence of each membrane length bin was assessed in each group and the number of gold particles adjusted according to the bin probability. This normalized data was plotted as a histogram to visually represent the distribution of gold particles (Fig. 3F and 3L). This analysis also revealed a highly different probability for the occurrence of DGL-α in the perisynaptic zone. This argues against the possibility that a change in the shape of spines accounts for the absence of DGL-α in the PSM, which is independently also supported by the observation that the similar subcellular distribution profile of another postsynaptic protein mGlu5 remained unchanged in *fmr1*$^{-/-}$ animals. To establish the average density of intracellular DGL-α labeling, first a background analysis was performed to assess the influence of randomly scattered gold particles on our sampling. Twenty five random asymmetrical synapses were imaged per animal, regardless of gold particle location (total n = 75). Presynaptic intracellular labeling was assumed to be true background. Density values were generated by calculating the number of gold particles found within this area and dividing by the total area, giving a value of gold particles/ μm^2. This background density value was subtracted from the density value of intracellular postsynaptic gold labeling of each animal, which was obtained by measuring the total surface area inside the spine heads and excluding the 40 nm thick zone below the plasma membrane.

For complete analysis of spine neck morphology, 75 images of intact spines receiving an asymmetric synapse were captured per animal regardless of size or labeling. Spines were classed as DGL-α positive or negative and the Chi^2 test used to assess statistical differences. Spine length was measured from the base of the neck to the furthest point on the spine head. Spine lengths were similar between animals of the same strain (Kolmogorov-Smirnov tests; $p > 0.05$), so data was pooled and compared between groups (Kolmogorov-Smirnov test; $p < 0.001$). Then all spines were separated into three compartments, spine head membrane, spine neck membrane and intracellular. Each compartment for each spine was classed as DGL-α positive or negative and the Chi^2 test used to calculate statistical differences. The area of each compartment, for each spine was generated and the density of gold labeling analysed by dividing the number of gold particles by the area. To assess the labeling at symmetrical GABAergic synapses, 50 synapses per animal were imaged regardless of size or labeling. Synapses were classed as DGL-α negative, or positive if a gold particle was found within 700nm of the synapse and the Chi^2 test used to assess statistical difference.

Finally, images were collected blind to the animal genotype and analyzed with Image J Software (National Institute of Health) and all statistics were performed using the STATISTICA analysis software.